# Beyond Conventional Inline Inspection: Passive Magnetic Field Evaluation for Pipeline Wall Loss

**Seamus Beairsto, Michael Byington, Shannon Campbell, Anouk van Pol,**

**John van Pol**

INGU Solutions Inc.


Organized by


*Proceedings of the 2024* **Pipeline Technology Conference** (ISSN 2510-6716).

*www.pipeline-conference.com/conferences*

# 1 ABSTRACT

This paper explores the use of passive magnetic flux density (MFD) for the characterization of metal loss in steel pipelines. Since the early development of MFL tools in the 1960s, the ferromagnetic properties of steel pipelines have been harnessed to determine the condition of pipelines with continuous development improving the resolution of these tools. However, the capability of low-resolution MFD analysis to inspect pipeline condition remains underexplored.

The machine learning powered Pipers® inline inspection solution (Michael Byington 2022), employs MFD analysis to identify pipe joints with potential metal loss exceeding 30 % of the nominal wall thickness. This approach provides an integrity assessment of pipelines with sufficient resolution to understand pipeline wall condition at least equivalent to hydrostatic tests.

This document discusses the passive magnetic field's properties, the development of a model for axially magnetized pipes, and the influence of external magnetic fields and non-cylindrical geometries on the passive magnetic field. It then demonstrates how, using this understanding of the passive MFD, the Pipers® solution can function as a low-resolution inline inspection tool, aiding in the safe and compliant management of pipelines. Finally, the approach is validated through comparisons with an MFL inspection.

Conclusively, this work showcases a novel analytical method for using passive MFD to detect metal loss in pipelines. By identifying segments at risk and guiding maintenance decisions, this low-resolution technique complements traditional high-resolution ILI tools, offering a strategic approach to pipeline management that emphasizes safety, compliance, and optimized resource allocation.

# 2 THE PASSIVE MAGNETIC FIELD OF A PIPE

INGU's Pipers® use microelectromechanical systems (MEMS) magnetometers to measure the passive magnetic field within ferromagnetic structures, such as pipelines. Pipers® are designed for deployment in two distinct configurations: free-floating, i.e. moving with the flow through the pipeline, or attached to an off-the-shelf cleaning pig (Matthew Kindree 2022).

Ferromagnetic materials exhibit long-range atomic-level ordering, causing unpaired electron spins to align parallel with each other in a region called a domain. While magnetization is intense within domains, the material typically remains unmagnetized on a bulk scale due to the random orientation of domains (Kittel 2005).

When exposed to an external magnetic field, like Earth's magnetic field, ferromagnetic materials can magnetize as domains align, significantly amplifying the induced magnetic field, a characteristic known as magnetic permeability. Mechanical strain can further induce magnetic anisotropy; for example, tensile stress on an iron crystal aligns the preferred magnetic direction with the stress, causing domain alignment (Schäfer 1998).

Observations reveal that pipeline pipes, due in part to their cylindrical geometry, tend to magnetize along their axial direction. This magnetization occurs spontaneously in the presence of Earth’s magnetic field and does not require a large, applied magnetizing field. Variations in mass and magnetic state, including external field strength, magnetic permeability, and magnetic history, induce variations in the axial magnetization, and by extensions the measured MFD (Kittel 2005).

## 2.1 MODELLING THE PASSIVE MAGNETIC FIELD

Utilizing Maxwell's equations and fundamental principles, we derive an equation describing the magnetic field along the centreline of a cylindrically symmetrical piece of pipe uniformly magnetized along the axial (y) direction (Figure 1). Equation 1 depicts the axial magnetic flux $B_y(y)$ along the y-axis, where $\mu_0$ represents the permeability of free space, and $M$ denotes the magnetic moment of the material, and $R$ represents the radius of the pipe (Griffiths 2013).

*Equation 1: Magnetic field of axially magnetized pipe*

$$B_y(y) = \frac{\mu_0 M}{2}\left(\frac{y-y_1}{\sqrt{(y-y_1)^2+R_{\text{out}}^2}} - \frac{y-y_2}{\sqrt{(y-y_2)^2+R_{\text{out}}^2}} + \frac{y-y_2}{\sqrt{(y-y_2)^2+R_{\text{in}}^2}} - \frac{y-y_1}{\sqrt{(y-y_1)^2+R_{\text{in}}^2}}\right)$$

The derivation of this equation is grounded in several assumptions:

1. There are no external magnetic fields present, with the sole magnetic field stemming from the magnetization of the pipe.
2. The pipe exhibits cylindrical symmetry.
3. The magnetization exhibits uniformity in the axial direction.

Empirical data shows only minor deviations indicating that this model is consistent with the dominant physical phenomena at play.

*Figure 1: Axially magnetized pipe.*

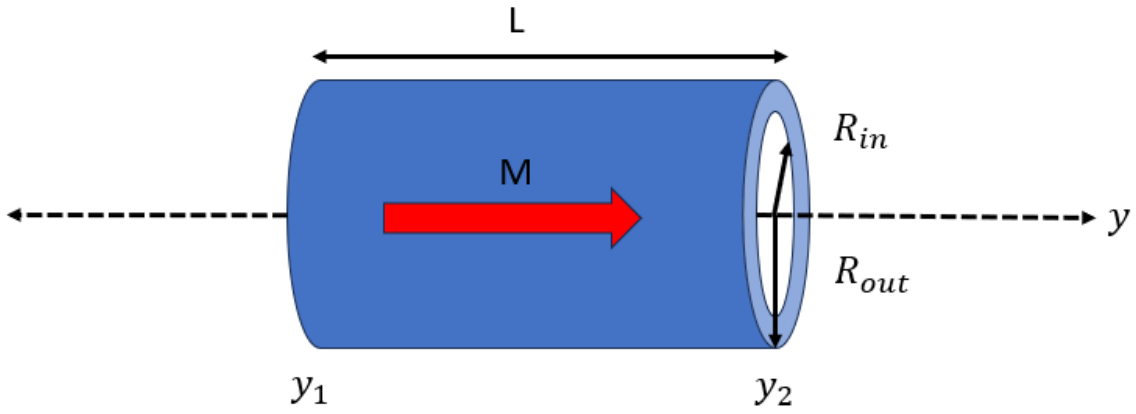


The additive nature of magnetic fields enables the use of Equation 1 to construct more complex scenarios. This approach allows the modelling of the axial magnetic field surrounding girth welds, where variations in material properties and stresses induce alterations in the pipe's magnetization.

*Figure 2: Three girth weld model.*

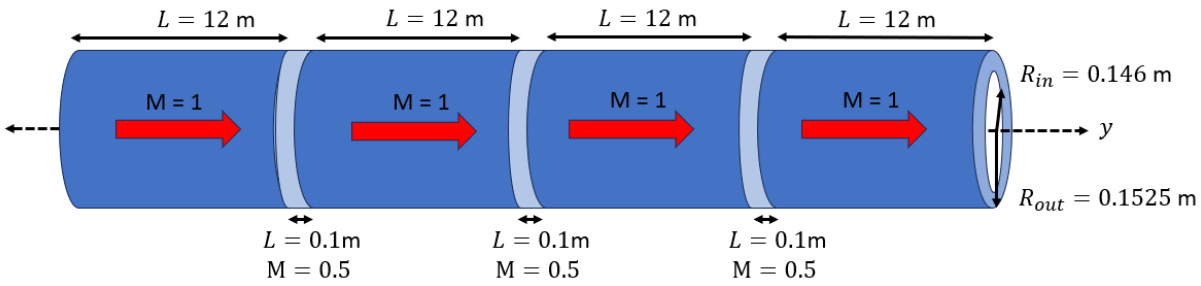


Figure 3 provides a comparative analysis: the top plot showcases a model representing four 12-metre-long pipe joints, with girth welds causing a reduction in axial magnetization Figure 2: Three girth weld model.Figure 2). This model is constructed by the summation of seven variants of Equation 1; four with $M = 1$ representing the pipe joints, and three with $M = 0.5$ representing the girth welds with a decreased axial magnetization. The bottom plot displays field data obtained from identical pipe joints. The match between our predictions and actual observations strongly supports our understanding of the pipe's basic magnetic properties.

*Figure 3: Girth weld signature, model vs. field data.*

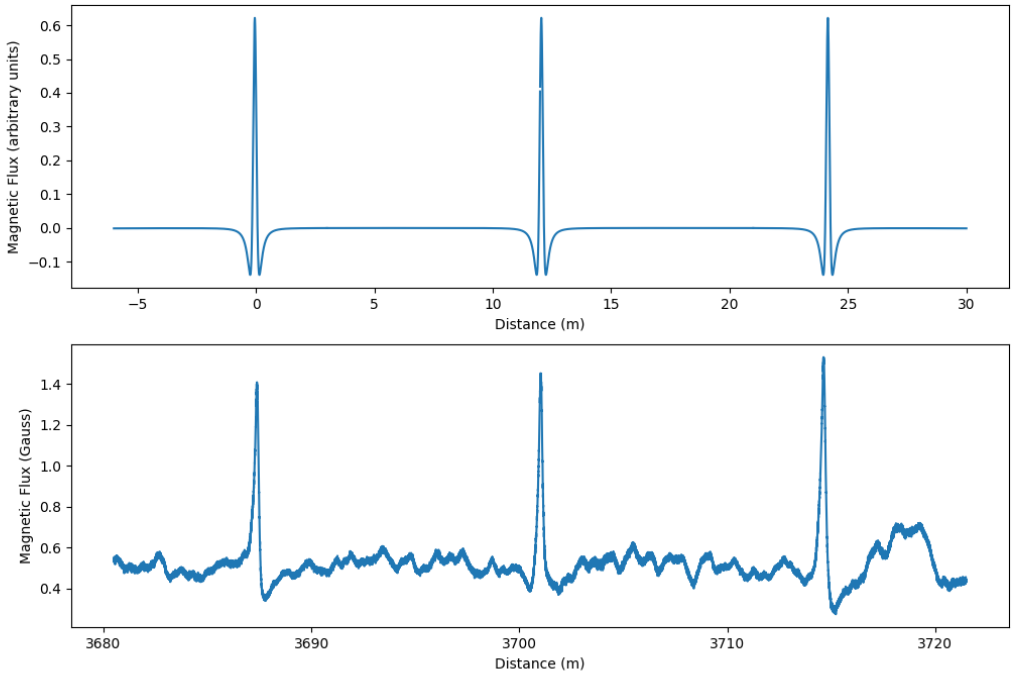


An implication of Equation 1 is that the magnetic field direction on the inside of an axially magnetized pipeline segment opposes the magnetization direction of the encompassing pipeline.

## 2.2 EFFECTS OF EXTERNAL MAGNETIC FIELDS

Building upon the foundation set by Equation 1, our model's first expansion integrates the impact of an external magnetic field on the passive magnetic field. Earth's magnetic field is ubiquitous and

exhibits global fluctuations typically ranging between 0.25 Gauss and 0.65 Gauss, with variations in declination and inclination dependent on geographic coordinates (William J. Hinze 2013). These parameters can be approximated as constant for a given pipeline location.

As previously mentioned, when exposed to an external magnetic field, like Earth's magnetic field, ferromagnetic materials can magnetize as domains align. Therefore, we hypothesise that alignment of the pipeline heading with Earth's magnetic field enhances the axial magnetization of the pipeline. Conversely, misalignment induces off-axial magnetization, diminishing axial magnetization.

To validate this hypothesis, we plot the alignment of the pipeline's orientation with Earth's magnetic field along with the measured MFD. Leveraging specified pipeline paths and elevation profiles, directional unit vectors are constructed for each pipeline segment. Subsequently, Earth's magnetic field's directional unit vector in the region of the pipeline is determined using magnetic declination and inclination. By projecting these unit vectors onto each other, the pipeline's alignment with Earth's magnetic field for each pipeline segment is determined.

*Figure 4: Axial magnetic flux vs. pipeline alignment with Earth's magnetic field.*

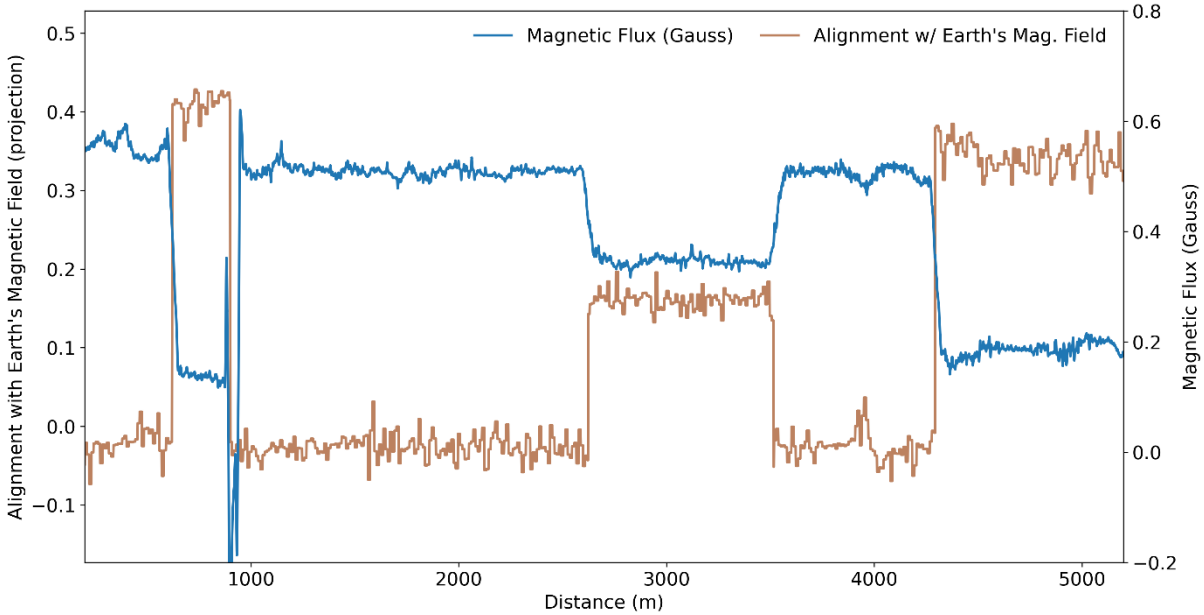


Building upon the foundation set by Equation 1, our model's first expansion integrates the impact of an external magnetic field on the passive magnetic field. Earth's magnetic field is ubiquitous and exhibits global fluctuations typically ranging between 0.25 Gauss and 0.65 Gauss, with variations in declination and inclination dependent on geographic coordinates. These parameters can be approximated as constant for a given pipeline location.

As previously mentioned, when exposed to an external magnetic field, like Earth's magnetic field, ferromagnetic materials can magnetize as domains align. Therefore, we hypothesise that alignment of the pipeline heading with Earth's magnetic field enhances the axial magnetization of the pipeline. Conversely, misalignment induces off-axial magnetization, diminishing axial magnetization.

To validate this hypothesis, we plot the alignment of the pipeline's orientation with Earth's magnetic field along with the measured MFD. Leveraging specified pipeline paths and elevation profiles, directional unit vectors are constructed for each pipeline segment. Subsequently, Earth's magnetic field's directional unit vector in the region of the pipeline is determined using magnetic declination

and inclination. By projecting these unit vectors onto each other, the pipeline's alignment with Earth's magnetic field for each pipeline segment is determined.

Figure 4 illustrates the impact of the pipeline's alignment with Earth's magnetic field on the axial MFD within the pipeline. Here we see a strong correlation between the axial magnetic field and the pipeline's alignment with Earth's magnetic field. The inverse relationship between the axial MFD and the pipeline's alignment with Earth's magnetic field aligns with the predictions derived from Equation 1. This relationship is indicative of heightened magnetization of the pipe wall along the direction of Earth's magnetic field causing a corresponding decrease in the MFD inside the pipeline, affirming the consistency between the empirical observation and the theoretical framework provided by Equation 1.

## 2.3 EFFECTS OF NON-CYLINDRICALLY SYMMETRIC GEOMETRY

Extending the model beyond the cylindrical symmetry assumed in Equation 1, we now include non-cylindrically symmetric geometries through a numerical approach. Our methodology begins with the development of a computer-aided design (CAD) model representing the desired geometry, such as a hot tap installed on the pipeline (Figure 5). This model is subsequently populated with magnetic dipoles aligned along the axial directions. In this context, the axial direction of the pipe body corresponds to the y-direction, while the axial direction of the hot tap aligns with the z-direction.

To determine the magnetic field along the centreline of the pipe, we employ the Biot-Savart law, as expressed in Equation 2:

*Equation 2: Biot-Savart Law*

$$\vec{B} = \frac{\mu_0}{4\pi}\left(\frac{3(\vec{m}\cdot\vec{r})\,\vec{r}}{r^5} - \frac{\vec{m}}{r^3}\right)$$

Here, $\vec{B}$ represents the vector describing the magnetic field, $\vec{m}$ denotes the vector representing the magnitude and orientation of the magnetic dipole, and $\vec{r}$ represents the vector describing the position of the dipole relative to the point where the magnetic field is being measured. To determine the MFD at any point, the contribution of each dipole is summed using Equation 2. This approach gives us not only a model of the axial magnetic field, but the radial component of the field as well.

*Figure 5: Hot tap model.*

Figure 6 presents a comparative analysis: The top plot showcases the magnetic field predicted by the CAD based model. The bottom plot displays field data obtained from the pipeline depicted in Figure

5, centred on the hot tap. Once again, we observe a strong resemblance between the model and field data.

*Figure 6: Hot tap model vs. field data.*

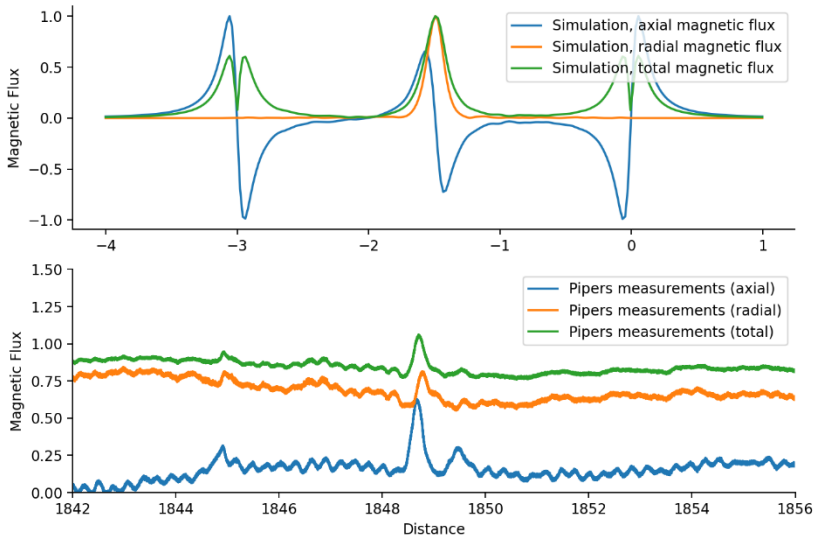


This approach enables a comprehensive assessment of magnetic fields in configurations beyond simple cylindrical symmetry, offering valuable insights into the magnetic behaviour of complex geometries such as the hot tap installation.

## 2.4 EFFECTS OF METAL LOSS ON THE PASSIVE MAGNETIC FIELD

Metal loss has a significant impact on the magnetic structure of the pipeline, thereby influencing the passive magnetic field detected by the Pipers® tool. This alteration in magnetic structure is influenced by several factors, including surface geometry, metal mass, and stress concentration zones (Kittel 2005).

While predicting the resultant magnetic structure based on first principles presents challenges, analysis of Pipers® data provides compelling evidence. It suggests that metal loss features with a minimum depth of 30% of the nominal wall thickness exhibit consistent behaviour. These features consistently produce a smooth localized decrease in both axial and radial MFD in the surrounding pipe, as depicted in Figure 8. Furthermore, there is a consistent overall decrease in axial and radial flux across the entire pipe joint compared to pipe joints in the surrounding pipeline, as illustrated in Figure 9.

These decreases in both axial and radial MFD are captured by the root-squared-sum of the magnetic components. This total MFD is depicted in green in Figure 6 and Figure 7.

*Figure 7: Localized decrease in the magnetic flux density around metal loss feature.*

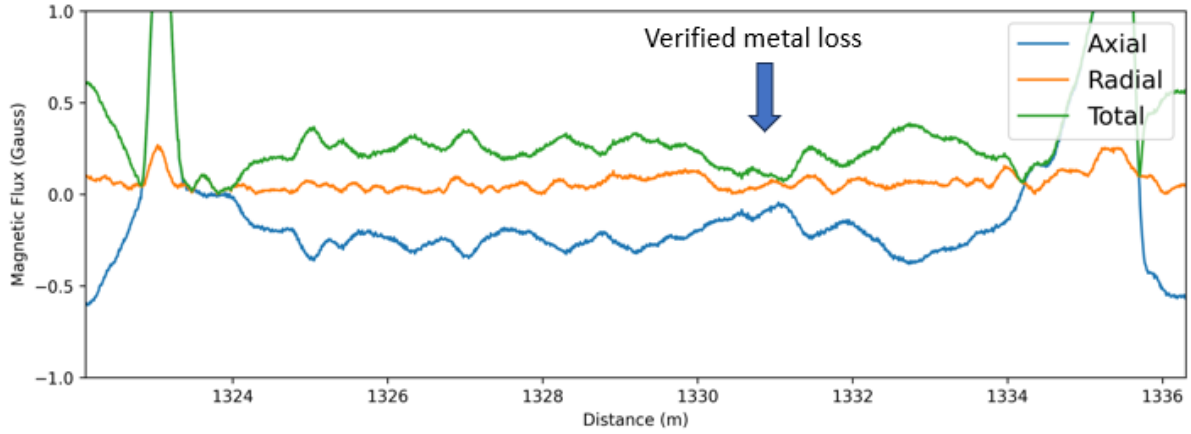

*Figure 8: Decreased average magnetic flux density in pipe joint containing a metal loss feature.*

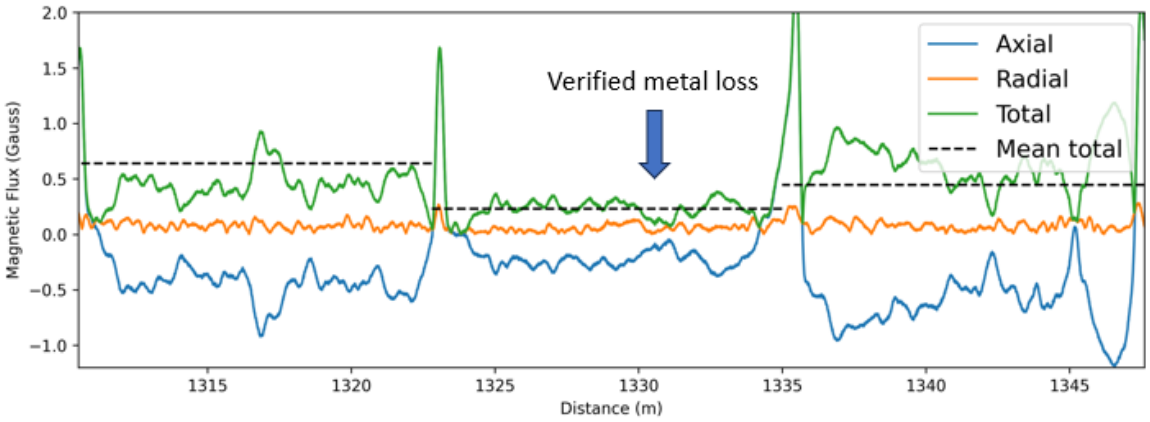


# 3 THE ANALYSIS

With an established understanding of the passive magnetic field within the pipeline and a corresponding measurement tool, we devise an analytical method to identify pipe joints likely to contain metal loss anomalies.

## 3.1 SEGMENTING THE PIPELINE

The initial step of the analysis involves segmenting the pipeline into sections with comparable baseline magnetic characteristics. Segmentation occurs based on changes in alignment with Earth's magnetic field (i.e. bends), changes in pipe diameter, and changes in nominal wall thickness.

Girth welds, with their distinct magnetic properties, are excluded from the analysis, with MFD within 1-metre on either side of each girth weld filtered out.

## 3.2 PIPE JOINT COMPARISON

Subsequently, we calculate the average total MFD within each pipe joint and compare it with the average total MFD of the parent pipeline segment. If the disparity exceeds an empirically determined threshold, which takes into account pipe diameter, wall thickness, and segment heading (N-S vs. E-W), the pipe joint is flagged as a potential candidate for containing a metal loss anomaly with a depth exceeding 30% of the nominal wall thickness.

## 3.3 SIGNATURE VETTING

Candidate locations undergo evaluation by a trained subject matter expert to distinguish MFD measurements attributable to metal loss from those associated with pipeline physical attributes (e.g. girth welds, bends, and anodes), or sensor noise. MFD measurements linked to metal loss are noted as metal loss anomalies in a feature list. Additionally, a confidence level is attributed to each metal loss anomaly, determined by factors such as how well the signal matches validated metal loss signatures, proximity to pipeline features that may distort the local magnetic structure, and the level of sensor noise around the location. This confidence level provides insight into the reliability of each identified anomaly, aiding in subsequent decision-making processes.

### 3.4 SUBSEQUENT DEPLOYMENTS

Due to the highly repeatable nature of Pipers® measurements of the MFD within a pipeline (R. Ho 2021), metal loss anomalies can be tracked over subsequent deployments. Through comparison with previous deployments, the rate of growth of a metal loss feature can be approximated, and metal loss features with the greatest growth rates can be identified.

## 4 VALIDATION

Figure 9 displays the validation of a Pipers® metal loss analysis, comparing the results of the metal loss analysis with metal loss features identified in an MFL inspection of the same pipeline. The severity density kernel for the MFL-detected metal loss features is shown in blue, quantified on the left-hand y-axis. This kernel is calculated by modelling each metal loss feature with a depth greater than 30 % of the nominal wall thickness by a Gaussian distribution, where the magnitude reflects the depth of the metal loss, and the half-width is based on the combined uncertainty of MFL and Pipers® linear distance measurements. Summing these Gaussian distributions forms the blue line, with individual MFL metal loss anomalies marked by blue points.

The confidence kernel for the Pipers®-detected metal loss features appears in red, with its magnitude indicated on the right-hand y-axis. It is calculated by representing each Pipers® metal loss feature as a Gaussian distribution, with the magnitude scaled to the feature's confidence level (low, medium, or high as confidence of 1, 2, or 3), and the half-width determined by the combined uncertainty of MFL and Pipers® linear distance measurements. The aggregation of these distributions results in the red line, with individual Pipers® metal loss anomalies shown as red markers.

*Figure 9: Validation of metal loss detection via measurement of the passive magnetic flux density.*

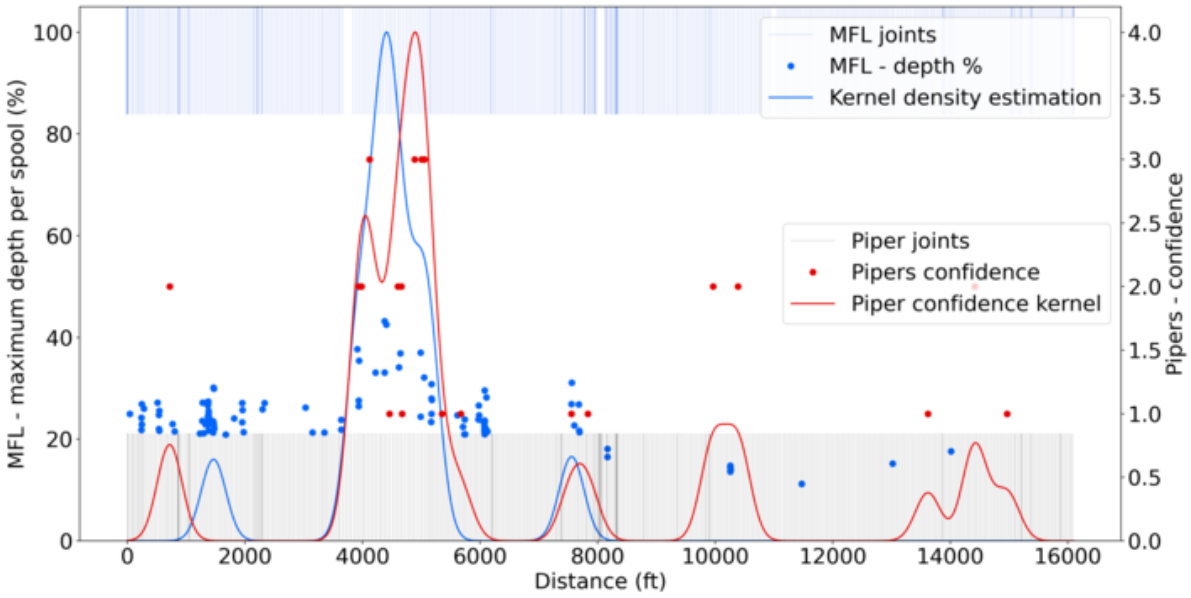


The overlap between the two kernels highlights the ability of the Pipers® metal loss analysis to accurately identify the pipeline segment in the poorest condition, as well as several other pipeline segments containing metal loss features. This method has received additional validation from clients through comparisons with traditional inline inspection tools.

# 5 CONCLUSIONS

This study presented a novel approach to detecting metal loss in steel pipelines through the analysis of passive magnetic flux density (MFD), leveraging the ferromagnetic properties of steel and the capabilities of the machine learning-enhanced Pipers® inline inspection solution. We detailed the theoretical underpinnings of passive MFD in steel pipelines, including the effects of external magnetic fields, non-cylindrical geometries, and metal loss on the magnetic field, and provided a comprehensive overview of the Pipers® technology's ability to detect significant metal loss.

The validation of our analytical framework through MFL comparisons and client feedback highlights its efficacy in accurately identifying severe metal loss anomalies and pinpointing segments of pipeline in poor condition.

Moreover, the versatility of this inspection approach extends beyond anomaly detection, offering practical applications in pipeline management. As an unconventional inline inspection tool, it provides an integrity assessment of pipelines with sufficient resolution to understand pipeline wall condition at least equivalent to hydrostatic tests. Additionally, it aids in identifying critical areas for localized high-resolution inspection, guides decision-making in dig planning for pipeline condition assessment, assists in the implementation of corrosion monitoring programs, and facilitates pipeline asset triage. Overall, the integration of passive MFD analysis into pipeline maintenance strategies holds significant promise for enhancing safety and compliance while optimizing resource allocation.

# 6 REFERENCES

Griffiths, David J. 2013. *Introduction to Electrodynamics.* Boston, MA: Pearson.

Kittel, Charles. 2005. *Introduction to Solid State Physics.* Hoboken, NJ: Wiley.

Matthew Kindree, Shannon Campbell, Anouk Van Pol, and John Van Pol. 2022. “Defect localization using free-floating unconvential ILI tools without AGMs.” *Pipeline Pigging and Integrity Management.* Houston, TX.

Michael Byington, Anouk van Pol, John van Pol. 2022. “Neural Networks for Pipeline Joint Detection.” *The Digital Pipeline Solutions Forum.* Houston.

R. Ho, Z. Shand, H.J. Son, and John van Pol. 2021. “Rapid Identification of New Hot Taps in Pipelines using Remnant Magnetism.” *Pipeline Pigging and Integrity Management Conference.* Houston.

Schäfer, Alex Hubert and Rudolf. 1998. *Magnetic Domains: The Analysis of Magnetic Microstructures.* Berlin: Springer-Verlag.

William J. Hinze, Ralph R. B. von Frese, Afif H. Saad. 2013. *Gravity and Magnetic Exploration: Principles, Practices, and Applications.* Cambridge: Cambridge University Press.